FABP7 is a key metabolic regulator in HER2+ breast cancer brain metastasis

Alex Cordero[1], **Deepak Kanojia**[1], **Jason Miska**[1], **Wojciech K. Panek**[1], **Annie Xiao**[1], **Yu Han**[1], **Nicolas Bonamici**[1], **Weidong Zhou**[2], **Ting Xiao**[1], **Meijing Wu**[1], **Atique U. Ahmed**[1], **Maciej S. Lesniak**[1]

[1]Department of Neurological Surgery, Northwestern University Feinberg School of Medicine, Chicago, IL 60611

[2]Center for Applied Proteomics and Molecular Medicine, George Mason University, Manassas, VA 20110.

Abstract

Overexpression of human epidermal growth factor receptor 2 (HER2) in breast cancer patients is associated with increased incidence of breast cancer brain metastases (BCBM), but the mechanisms underlying this phenomenon remain unclear. Here, to identify brain-predominant genes critical for the establishment of BCBM, we conducted an *in silico* screening analysis and identified that increased levels of fatty acid binding protein 7 (FABP7) correlate with lower survival and higher incidence of brain metastases in breast cancer patients. We validated these findings using HER2+ BCBM cells compared to parental breast cancer cells. Importantly, through knockdown and overexpression assays we characterized the role of FABP7 in the BCBM process *in vitro* and *in vivo*. Our results uncover a key role of FABP7 in metabolic reprogramming of HER2+ breast cancer cells, supporting a glycolytic phenotype and storage of lipid droplets that enable their adaptation and survival in the brain microenvironment. Additionally, FABP7 is shown to be required for up-regulation of key metastatic genes and pathways, such as Integrins-Src and VEGFA, and for the growth of HER2+ breast cancer cells in the brain microenvironment *in vivo*. Together our results support FABP7 as a potential target for the treatment of HER2+ BCBM.

Keywords

Breast cancer brain metastasis (BCBM); HER2; FABP7; metabolic reprogramming

---

Corresponding author: Correspondence and requests for materials should be addressed to Dr. Maciej S. Lesniak, M.D. Department of Neurological Surgery, Northwestern University Feinberg School of Medicine, 676 N. St Clair Street, Chicago, Illinois 60611. Telephone: (312) 926-1094. Fax: (312) 695-3294. maciej.lesniak@northwestern.edu.

AUTHOR CONTRIBUTIONS

Author contributions: A.C.: conception and design, collection and/or assembly of data, data analysis and interpretation, manuscript writing, and editing of manuscript. D.K.: conception and design, data analysis and interpretation, and editing of manuscript. J.M., W.K.P., A.X., Y.H., N.B., Z.W., A.A.,T.X., M.W.: collection and/or assembly of data and final approval of manuscript. M.S.L.: conception and design, financial support and final approval of manuscript.

Conflict of interest: The authors declare no potential conflict of interest.

INTRODUCTION

Central nervous system (CNS) metastases are a late complication of many solid tumors. Breast cancer represents a leading cause of brain metastasis, second to lung cancer (1). Brain metastases occur in about 25–50% of breast cancer patients and limits their median survival to less than 10 months (1, 2). Factors that increase the likelihood of brain metastases are still under investigation; however, amplification of the human epidermal growth factor receptor 2 (*HER2*) gene, present in 20–30% of breast cancers (3), is known to be associated with decreased overall patient survival and increased metastasis to bone, lungs, liver, and brain (4, 5). Systemic therapies such as trastuzumab (6) are thwarted by the blood-brain barrier (BBB) and leave clinicians with a limited arsenal to effectively treat breast cancer brain metastases (BCBM). Therefore, the need to discover additional means to target HER2+ BCBM is large.

To develop effective treatments against BCBM it is crucial to understand its biology. Recent studies using paired parental/BCBM models identified overexpression of neuronal markers, such as ST6GALNAC5 (ST6), Nestin/CD133, GABA receptor and neuroserpin, in BCBM cells (7–10). The overexpression of these genes by brain metastatic cells supports their adaptation to survive and thrive in the brain microenvironment. However, the active role of these brain predominant markers in conferring BCBM has not been evaluated.

The metastatic process has unique metabolic demands critical for the adaptation and survival of tumor cells when attempting to seed in a new environment (11). Indeed, the metabolic reprogramming is now widely recognized as a hallmark of cancer and confers cells the ability to meet energetic and biomass demands. Cancer cells are known to adopt a glycolytic phenotype in the presence of oxygen despite the lower efficiency in ATP generation (12). The advantage of this metabolic reprogramming, termed the "Warburg effect", is that it yields metabolic products to promote proliferation and cell growth. In addition to reprogramming of glucose metabolism, cancer cells can also promote fatty acid metabolism and uptake to support their proliferation and metastatic potential (13–17). However, the intricacies for this tumor cell adaptation are not entirely understood. Fatty acid binding proteins (FABPs) are proposed to be central regulators of lipid metabolism and energy homeostasis due to their function in regulating fatty acid uptake and intracellular lipid droplet formation (18). Lipid droplets are hubs for the energy and lipid metabolism, and in cancer serve to protect malignant cells from reactive oxygen species and support their survival during reoxygenation post-hypoxia (19). Consequently, such regulation of fatty acid transport and storage may be one of the ways cancer cells ensure their survival.

In the present study, we have identified that overexpression of the Fatty acid binding protein 7 (*FABP7*), a brain-specific intracellular lipid binding protein, correlates with poor survival and is associated with increased incidence of brain metastases in breast cancer patients. Notably, using *in vitro* and *in vivo* studies, we show that FABP7 plays a crucial role in establishing HER2+ BCBM, through regulation of cell invasion and metabolic reprogramming that favors a glycolytic phenotype, promoting the adaptation and survival of BCBM in the brain microenvironment. Cumulatively, our results support the specific targeting of FABP7 agaits HER2+ BCBM.

RESULTS

FABP7 is overexpressed in patients with breast cancer brain metastases.

Previously published reports indicate an increased amount of neuronal markers overexpression in BCBM (7–10). Therefore, we aimed to identify novel potential target genes required for the formation of BCBM. For this, we performed an *in-silico* screening using publicly available microarray data sets (NKI Breast Cancer Data (20) and GSE (GSE19536, GSE14020) data sets. Analysis of the human breast cancer survival and metastasis databases (20, 21), identified *FABP7* as a potential brain-predominant gene correlated with poor prognosis in breast cancer patients (Supplementary Table S1). Next, breast cancer patients were divided into *FABP7* high and low expression groups at a cut-off value of 0.548 determined by recursive partitioning analysis (22). Patients showing high levels of *FABP7* presented significantly reduced survival rates compared to patients with lower levels of *FABP7* (Fig. 1A). Within breast cancer patients, *FABP7* was found to be significantly increased in HER2+ and Basal/ triple-negative breast cancer (TNBC) patients, compared to patients with luminal-like breast cancer (GSE19536) (Fig. 1B and Supplementary Fig. 1A). In a separate analysis, *FABP7* was shown to be significantly higher in breast cancer patients with brain metastases compared to patients with metastases to the lungs and bones (GSE14020) (Fig. 1C). Next, we evaluated the expression levels of 33 brain-predominant genes associated with poor prognosis in breast cancer patients (Supplementary Table S1) by qRT-PCR using paired parental/BCBM HER2+ and TNBC models (Supplementary Fig. 1B). Our results showed a significant *FABP7* upregulation in BT474 brain-seeking (Br) cells, a HER2+ cell line with an increased ability to metastasize to brain (23), compared to parental BT474 cells. In contrast, triple-negative MDA231-Br BCBM cells showed no significant difference for *FABP7* expression compared to the parental MDA231 cells. In this model, *TUBB3* expression was significantly upregulated in MDA231-Br cells, as previously described (24). Notably, no significant differences in the expression of any other brain-predominant gene were found between paired parental/BCBM cells (Supplementary Fig. 1B).

Next, we analyzed the expression of FABP7 in different subtypes of breast cancer cell lines by Western blot. FABP7 was detected in two HER2+ breast cancer cell lines, whereas luminal-like breast cancer and TNBC subtypes showed no FABP7 expression *in vitro* (Supplementary Fig. 1C). Importantly, FABP7 levels were increased in HER2+ BT474-Br cells compared to BT474 cells, whereas no differences were seen between paired TNBC MDA231/MDA231-Br and CN34/CN34-Br cells *in vitro* (Fig. 1D–F).

In order to assess the expression levels of FABP7 *in vivo*, two different HER2+ (BT474-Br or BT474 and HCC 1954) and TNBC (MDA231-Br and CN34-Br) breast cancer cell lines were injected either intracranially or orthotopically in the 3rd and 4th mammary gland of nude mice. Mammary glands and brains were harvested from mice at the study end-time points, as described in the Methods. Histopathologic analysis confirmed the formation of tumors in the brain and mammary glands for both *in vivo* models (Supplementary Fig. 2 A, B). As expected, we confirmed a strong HER2 expression in BT474-Br, BT474 and HCC 1954 tumors, whereas no HER2 expression was found in TNBC tumors (Fig. 1G,

Supplementary Fig. 2B). Remarkably, our results showed high expression levels of FABP7 in BT474-Br and HCC 1954 tumors grown in the brain microenvironment, compared to BT474 and HCC 1954 tumors formed in the mammary glands (Fig. 1G, Supplementary Fig. 2B). Although triple negative CN34-Br tumors formed in the brain microenvironment also expressed FABP7, this expression was absent in CN34-Br tumors formed in the mammary gland, and not as prominent as in HER2+ breast cancer cells grown in the brain (Fig. 1G, Supplementary Fig. 2A, B). Additionally, no FABP7 expression was detected in MDA231-Br tumors grown in either brain or mammary glands (Fig. 1G, Supplementary Fig. 2A, B).

Together, these results suggest that FABP7 might play an important role in the formation of BCBM in HER2+ breast cancer patients, thus in further studies we focused in investigating the role of FABP7 in HER2+ breast cancer.

FABP7 promotes HER2+ BCBM cell invasion *in vitro*.

In order to understand the functional role of FABP7 in BCBM, we stably knockdown *FABP7* expression via lentiviral transduction using shRNAs (sh1 and sh2) in two different HER2+ breast cancer cell lines: BT474-Br and HCC 1569 (Fig. 2A,B, Supplementary Fig. 3A). No morphological differences or changes in cellular proliferation or apoptosis were observed between *FABP7* knockdown (KD) BT474-Br or HCC 1569 cells and the respective controls *in vitro* (Supplementary Fig. 3B–D).

The tumor cell metastatic cascade is a unique multi-stage process where cell invasion is a key trigger factor for cancer progression and metastasis to distant organs (25). In this context, previously published data revealed that FABP7 downregulation is associated with decreased tumor cell invasion in melanoma cell lines (26). In order to evaluate the role of FABP7 on the invasion ability of metastatic breast cancer cells, *in vitro* matrigel invasion assays were performed. Our results demonstrated a significant reduction in invasion of *FABP7* KD BT474-Br cells, by 36% (± 10) for sh1 and 80.5% (± 3) for sh2 cells, respectively, compared to control cells (Fig. 2C).

To confirm these results and the role of *FABP7* in invasion of breast cancer cells, we overexpressed *FABP7* using a pLVX lentiviral vector containing full-length *FABP7* in parental BT474 cells. FABP7 overexpression (OE) was confirmed at both protein and RNA levels (Fig. 2D). Our data showed a significant increase in the number of invading cells after *FABP7* overexpression, compared to vector control cells (Fig. 2E). Similarly, knockdown of *FABP7* in HCC 1569 cells significantly decreased the number of invasive cells compared to control (Supplementary Figure 3E), whereas *FABP7* OE in HCC 1954 cells slightly increased the invasion ability of these cells compared to control cells (Supplementary Figure 3F,G).

Together, these results support a role for *FABP7* in promoting invasion of HER2+ breast cancer cells.

FABP7 controls expression of metabolic and invasion-related proteins in HER2+ BCBM cells.

In order to determine the effects of targeting *FABP7* on protein expression in HER2+ BCBM cells, lysates from control and *FABP7* KD BT474-Br cells were subjected to liquid chromatography tandem mass spectrometry (LC-MS/MS) using LTQ-Orbitrap. The Proteasome Discoverer™ search results were filtered by stringent criteria, which yielded 8687 proteins (including homologous isoforms). Based on the MS spectra count (Supplementary Table S3A), relative quantitative analysis of the identified proteins revealed that 256 proteins were significantly differentially expressed in *FABP7* KD BT474-Br cells compared to control cells (Supplementary Table S3B). We then performed gene ontology analysis on these proteins, which showed that proteins associated with the glycolytic process were significantly altered in *FABP7* KD BT474-Br cells compared to control cells (Fig. 3A). This analysis also indicated that the expression of proteins affected by *FABP7* KD in BT474-Br cells were associated with tumor cellular movement, cell death and survival, post-translational modifications, protein folding and nucleic acid metabolism (Fig. 3A). Interestingly, our results showed that the expression levels of mitochondrial precursors, regulators, interactors and oxidative phosphorylation (OXPHOS) - related proteins were significantly increased in *FABP7* KD BT474-Br cells compared to control cells (Fig. 3 B,C). In addition, proteins involved in glycolytic processes were found to be significantly downregulated in FABP7 *KD* BT474-Br cells compared to control cells (Fig. 3 D,E). These results suggest that FABP7 plays an important role in the regulation of metabolic reprogramming in HER2+ BCBM cells.

Additionally, consistent with a potential role for FABP7 in promoting invasion of HER2+ BCBM cells (Fig. 2C,D and Supplementary Fig. 3E,G), our mass spectrometry results also revealed a significant decrease in the levels of invasion-related proteins in *FABP7* KD BT474-Br cells compared to control cells (Fig. 3F). Conversely, the expression of tight junction-related proteins, critical for the maintenance of the mammary epithelial cells interaction and prevention of metastasis (27), were found to be significantly increased in *FABP7* KD BT474-Br cells compared to control cells (Fig. 3F,G). Consistently, ZO-2 expression was found to be decreased in *FABP7* overexpressing BT474 cells compared to controls (Fig. 3G).

Together, these results support a potential role for FABP7 as a regulator of cell metabolic reprogramming and metastatic/invasive ability in HER2+ BCBM cells.

FABP7 controls metabolic reprogramming in HER2+ BCBM cells

Metabolic reprogramming is a hallmark of cancer, providing energy and substrates for various biosynthetic processes to facilitate cancer cell growth and survival under hypoxic or nutrient-scarce conditions (28). Given our mass spectrometry results, indicating a potential role for FABP7 as a regulator of cellular metabolism, we next analyzed how alterations in *FABP7* expression can influence the metabolic properties of HER2+ BCBM cells *in vitro*.

Extracellular flux analysis measuring oxygen consumption rate (OCR) is a powerful tool for the study of OXPHOS in cells (29), and was used to quantify the effect of *FABP7* KD on

OCR of HER2+ BCBM cells. Notably, the basal OCR levels (reflecting basal mitochondrial activity) were significantly increased in *FABP7* KD BT474-Br cells compared to control cells (Fig. 4A, Supplementary Fig. 4A). Treatment of cells with carbonyl cyanide-*4*-(trifluoromethoxy)phenylhydrazone (FCCP) allows the measurement of maximal OCR. Upon FCCP treatment, *FABP7* KD BT474-Br cells showed a significant increase in the maximal OCR when compared to control cells (Fig. 4A,B), indicating that knocking down *FABP7* in HER2+ BCBM results in a significant enhancement of OXPHOS metabolism. Reduction in OCR after oligomycin treatment is a direct measurement of ATP-linked respiration of cells (30), and our results showed that *FABP7* KD BT474-Br cells generate significantly higher mitochondrial-dependent ATP levels as compared to control cells (Fig. 4B). The same effects were observed when we knocked down *FABP7* in HCC 1569 cells (Supplementary Fig. 4B,C). Additionally, further supporting a key role for FABP7 as a regulator of mitochondrial metabolism in HER2+ breast cancer cells, overexpression of *FABP7* in BT474 and HCC 1954 cells significantly decreased not only the basal and maximal OCR, but also the amount of mitochondrial-dependent ATP synthesis, compared to respective control cells (Fig. 4 A,B and Supplementary Fig. 4B,C). Together, these results suggest that FABP7 acts as a negative regulator of OXPHOS metabolism and production of ATP in the mitochondria.

Adaptation to hypoxia by the metabolic reprogramming of tumor cells is an important cellular process required for the growth and survival of breast cancer metastatic cells in the brain microenvironment (31, 32). In order to investigate how FABP7 expression could affect the metabolic adaptation of HER2+ breast cancer cells in the brain, we cultured control, *FABP7* KD, and *FABP7* OE HER2+ breast cancer cells under hypoxia conditions *in vitro* (1% O_2, 5% CO_2, 37°C) and measured the Extracellular acidification rate (ECAR). Interestingly, there was a significant decrease in the glucose stimulated ECAR and the glycolytic capacity in *FABP7* KD BT474-Br cells grown under 24h-induced hypoxic and normoxic (20.7% O_2, 5% CO_2, 37°C) conditions, compared to BT474-Br control cells (Fig. 4C, Supplementary Fig. 4D). In contrast, *FABP7* OE in BT474 cells induced a significant increase in glycolysis under hypoxia when compared to BT474 control cells. These results suggest that FABP7 favors the glycolytic process in HER2+ breast cancer cells.

Hypoxia in tumor cells is known to induce the formation of lipid droplets (LD), cellular organelles that aid in the regulation of intracellular lipid storage and metabolism (33). In order to determine if *FABP7* induces changes in the lipid metabolic pathway, we analyzed the levels of fatty acid oxidation (FAO) in *FABP7* KD and control BT474-Br cells using extracellular flux analysis (Fig. 4D). Palmitate-BSA and oleate-BSA were injected to measure lipid-oxidation, and BSA injection was used as control. Interestingly, our results revealed a significant increase in both palmitate and oleate-induced OCR in *FABP7* KD BT474-Br cells in hypoxia, compared to BT474-Br control cells (Fig. 4D). No differences were seen after BSA injection (Supplementary Fig. 4E) or in normoxic conditions (Supplementary Fig. 4F) between these cell lines. Notably, we found a significant decrease in the formation of LD in *FABP7* KD BT474-Br cells and *FABP7* KD HCC 1569, compared to respective control cells, grown under normoxic and hypoxic conditions (Fig. 4E,F, Supplementary Fig. 4G).

Taken together, these results suggest that FABP7 might act as an important metabolic switch that supports the adaptation and survival of HER2+ breast cancer cells in the brain.

FABP7 promotes integrin-Src signaling and expression of proangiogenic factors in HER2+ BCBM cells.

Focal adhesion kinase (FAK) and Src family of protein tyrosine kinases coordinate multiple signaling pathways involved in tumor progression (34). Their hyperactivation in tumor cells, downstream of the integrin family of cell adhesion receptors, promotes proliferation, survival, angiogenic and metastatic events (34). Thus, we next evaluated whether FABP7 plays a role in activation of the integrin-FAK-Src signaling pathway under normoxic and hypoxic conditions. Our results showed that knockdown of *FABP7* in BT474-Br cells resulted in decreased phosphorylation of FAK at Tyr394 (Fig. 5A) and Src at Tyr416 under both normoxia and hypoxia conditions compared to control cells. Notably, the levels of hypoxia-inducible factor 1-alpha (HIF1α), a protein that influences cancer cell function, alters the extracellular matrix (ECM), and increases angiogenesis (35), were also found to be markedly decreased in *FABP7* KD BT474-Br cells compared to control cells under hypoxia treatment (Fig. 5A). In contrast, *FABP7* OE in BT474 cells increased both FAK and Src activation in normoxia conditions compared to control cells, and also led to an increase in phosphorylation of Src under hypoxia conditions.

Metastatic cell growth in the brain demands a sufficient degree of neovascularization to satisfy the oxygen and nutrient needs of the tumor mass (32). Thus, we next analyzed the expression of the proangiogenic vascular endothelial growth factor A (*VEGFA*) and Prolyl 4-Hydroxylase Subunit Alpha 1 (*P4HA1*), a VEGFA regulator that also regulates the ECM remodeling in response to hypoxia (36, 37). Our results showed an increase in *VEGFA* and *P4HA1* levels in both BT474-Br control and *FABP7* KD BT474-Br cells after induction of hypoxia for 12h and 24h compared to normoxic conditions (Fig. 5B). However, the induction of both angiogenic markers upon hypoxia treatments in *FABP7* KD BT474-Br cells was significantly reduced compared to BT474-Br control cells. Moreover, hypoxia-induced *VEGFA* and *P4HA1* levels were significantly increased in BT474 cells overexpressing *FABP7* compared to BT474 control cells (Fig. 5B). Similar findings were obtained using *FABP7* KD HCC1569 and *FABP7* overexpressing HCC1954 cells compared to respective controls (Supplementary Fig. 5).

Taken together, these results support an essential role for FABP7 in the regulation of key signaling molecules which are involved in the process of BCBM.

FABP7 is required for the formation of HER2+ BCBM *in vivo*

As our results show that *FABP7* knockdown in BCBM cells alters *in vitro* tumor cell invasion, metabolic reprogramming and pro-metastatic signaling pathways, we next sought to determine the role of FABP7 *in vivo* using preclinical models of BCBM.

In initial studies, BT474-Br, *FABP7* KD BT474-Br, BT474 and *FABP7* OE BT474 cells were injected intracranially in nude mice, and survival was monitored. Mice in the BT474-Br control group exhibited a median survival of 62 days, whereas only one mouse in the *FABP7* sh1 KD BT474-Br group died at day 112 and none of the mice in the *FABP7* sh2

KD BT474-Br group died throughout the length of our study (Fig. 6A, left panel). On the other hand, mice in the *FABP7* OE BT474 group presented a significant decrease in survival compared to BT474 control group (Fig. 6A, right panel). Histopathologic analysis of brain sections harvested from mice from each group, confirmed the formation of a tumor mass in the brains of mice in the BT474-Br, BT474 and *FABP7* OE BT474 groups, and in the brain of the mouse that died in the *FABP7* sh1 KD BT474-Br group (Fig. 6B, upper panels). No tumor formation was observed in the brain of the rest of the mice in *FABP7* sh1 and sh2 KD BT474-Br groups (Fig. 6B, upper panels, representative picture from sh2 group). Moreover, high levels of FABP7 were found to be expressed in the tumors formed in the brain of mice from the BT474-Br, BT474, and *FABP7* OE BT474 groups by immunofluorescence analyses (Fig. 6B, lower panels). Interestingly, FABP7 levels in the tumor developed in the brain of the mouse that died in the *FABP7* sh1 KD BT474-Br group were similar to the FABP7 levels observed in the BT474-Br control group (Fig. 6B), whereas FABP7 levels were almost absent in the brain sections from *FABP7* sh1 and sh2 KD BT474-Br groups with no tumors (Fig. 6B, lower panel, representative picture from sh2 group).

Notably, in *in vitro* assays, we observed a marginal difference in proliferation between *FABP7* KD BT474-Br and *FABP7* OE BT474 cells compared to the respective control cells under normoxia and hypoxia conditions (Supplementary Fig. 6), similar to what was shown under normal conditions (Supplementary Fig 2C). Thus, differences in proliferation between these cells do not seem to be the driver of the differences in survival observed in our *in vivo* studies.

Next, we sought to determine whether overexpression of FABP7 plays a role in tumor growth in the primary site. For this, BT474 and *FABP7* OE BT474 cells were orthotopically injected in the 3rd and 4th mammary gland of nude mice and tumor volume was monitored. There were no differences in mammary tumor growth observed between control and *FABP7* OE BT474 group (Supplementary Fig. 7A). Successful overexpression of *FABP7* in the tumors developed in mice from the *FABP7* OE BT474 group was confirmed by immunofluorescence analysis in comparison to tumors isolated from mice in the BT474 control group (Supplementary Fig. 7B). Together, our *in vivo* studies suggest that FABP7 plays a specific role in the tumor growth of breast cancer cells in the brain microenvironment.

In order to better understand the functional role of FABP7 on the metastatic behavior of breast cancer cells *in vivo*, BT474 and *FABP7* OE BT474 cells were injected systemically via an intracardiac route, and BCBM formation was determined by *in vivo* bioluminescence imaging (BLI). Our results showed that only 9% of the mice injected with BT474 control cells developed brain metastases 12 weeks after injection, whereas BCBM incidence was significantly increased to 64% in mice injected with *FABP7* OE BT474 cells (Fig. 6C). Moreover, the BLI intensity in *FABP7* OE BT474 group was significantly increased compared to control BT474 group (Fig. 6C).

Taken together, these results support a role for FABP7 as a key regulator of HER2+ BCBM formation, at least in part, through controlling the adaptation and survival of breast cancer cells in the brain microenvironment.

DISCUSSION

Brain metastasis is a major cause of mortality in breast cancer patients, and there is an urgent need to determine molecular targets for the treatment of breast cancer brain metastases. This study's aim was to identify potential targetable brain-predominant genes ectopically expressed in breast cancer cells, which enable their adaptation and growth within the brain microenvironment. Our results identified FABP7 as a key regulator of brain metastatic potential of HER2+ breast cancer cells by promoting tumor cell invasion, expression of angiogenesis regulators, and integrin-Src signaling pathway. Furthermore, we demonstrate that FABP7 controls the metabolic reprogramming of HER2+ breast cancer cells, events previously shown to be essential for adaptation, survival and growth of metastatic cells in the brain microenvironment (38), and is required for the establishment and growth of HER2+ BCBM in the brain. In contrast, although FABP7 expression is increased in Basal/TNBC patients compared to luminal-like breast cancer patients, this protein seems to have a less prominent role in the formation of TNBC brain metastases, as CN34-Br and MDA231-Br cells do not show increased expression of FABP7 compared to the parental cells *in vitro*, and FABP7 expression was either absent or low in TNBC-Br cells grown in the brain microenvironment.

FABP7 is a brain-specific intracellular lipid binding protein expressed primarily in radial glial cells during development (39). This protein belongs to a large family of hydrophobic ligand-binding proteins that promote cellular uptake and transport of fatty acids, regulation of metabolic pathways, gene expression, and cellular growth (40, 41). Previous studies described the role of other members of this superfamily of binding proteins in the progression and metastasis of different tumors, including FABP3 in non-small cell lung cancer (42) and FABP4 and FABP5 in TNBC, prostate, colorectal and ovarian cancer (43). Additionally, overexpression of FABP7 has been previously associated with increased tumor cell migration and invasion in glioma cell lines, and reduced survival in grade IV astrocytoma, glioblastoma multiforme, melanoma and renal cell carcinoma patients (26, 44–46). Recent impactful studies have shown that increased expression of different FABP family members, including FABP4, FABP5 and FABP7, are important to breast cancer development and progression (47–51). Specifically, these studies demonstrate that circulating FABP4 (47) or stromal expression of FABP4 and FABP5 (48, 51) can directly promote breast carcinogenesis by enhancing breast cancer cell proliferation and interaction with the surrounding microenvironment. Supporting these findings, here we demonstrate that *FABP7* overexpression correlates with poor overall survival in breast cancer patients and is upregulated in HER2+ and TNBC breast cancer patients compared to luminal-like breast cancer patients, which have a better disease prognosis. In addition, we show that *FABP7* is up-regulated in breast cancer patients with brain metastases compared to patients with metastasis to other organs. Notably, FABP7 expression was not detected in breast cancer tumors grown in the primary site, whereas its levels were up-regulated when TNBC CN34-Br and HER2+ breast cancer tumors grew in the brain, supporting a potential role of FABP7 for adaptation and survival of breast cancer cells in this microenvironment. Importantly, the expression of βIII tubulin (*TUBB3*) a brain-predominant gene that we have previously

identified as important for formation of BCBM (24), was also associated with poor breast cancer patient survival in our screening.

In order to progress and disseminate to secondary organs, a metastatic tumor cell must acquire invasive properties. Invasion of breast cancer cells depends on the interaction of cancer cells with the ECM, activation of several signaling pathways, such as the integrin-mediated FAK-Src, PI3K-Akt and MAPK pathways, and expression of several mediators of angiogenesis and invasion processes (36, 52–54). Our results demonstrate that FABP7 enhances the invasive ability of HER2+ breast cancer cells *in vitro* and the formation of brain metastasis *in vivo*, possibly through activation of the FAK-Src signaling pathway, overexpression of angiogenic and invasion markers, such as HIF1α, VEGFA and P4HA1, and downregulation of tight-junction-related proteins, such as ZO-2. The expression of tight-junction-related proteins is critical for the maintenance of cell-cell interactions, cellular polarization, ECM remodeling, and prevention of breast cancer metastasis (27, 55–58). Indeed, reduction of ZO-2 levels has been previously associated with metastasis of breast tumor cells (59). In addition, knockdown of P4HA1, a critical regulator of ECM remodeling, collagen biosynthesis and VEGFA expression, in breast cancer cells completely blocks spontaneous metastasis (36, 37).

Energy metabolism is one of the main processes affected during the transition from healthy to cancer cell, as cancer cells preferentially utilize glucose rather than mitochondrial OXPHOS to generate energy, even in the presence of oxygen (Warburg effect) (60). Aerobic glycolysis is critical for the tumor cell to metastasize and adapt to survive in the brain microenvironment (61–63). Our results indicate that FABP7 plays a critical role in the metabolic shift in HER2+ breast cancer cells. Through proteomic analysis we found a significant reduction in several glycolytic-related proteins, such as pyruvate kinases (PKM and PKLR) and fatty acid synthase (FASN), in *FABP7* KD BCBM cells compared to control cells. Previous studies support the importance of the regulation of these genes in tumor cell progression, migration/invasion and metastasis (64–66). In agreement with these observations, FABP7 overexpression in HER2+ breast cancer cells results in enhanced glycolytic metabolism, while *FABP7* knockdown limited ECAR rate in HER2+ BCBM cells. This strongly suggest that FABP7 has positive effects on glycolytic metabolism, which is important in primary and brain metastatic breast cancer cells (31, 67).

Conversely to decreased the glycolytic metabolism in *FABP7* KD cells, we revealed an increase in the expression of mitochondrial precursors, interactors and OXPHOS-related proteins in *FABP7* KD BCBM cells. Analysis of OCR, a powerful tool for the study of mitochondrial function in cells (29), confirmed that FABP7 limits both basal and maximal mitochondrial respiration in HER2+ breast cancer cells. Furthermore, we found that FABP7 KD in HER2+ BCBM cells increased oxidation of fatty acids and decreased production of lipid droplets, highlighting the crucial role for FABP7 in the regulation of lipid metabolism in these cells. These compelling results suggest that FABP7 acts as a direct gatekeeper for lipid OXPHOS. By seizing lipids and shuttling them to LD, FABP7 appears to prevent excessive OXPHOS or maintain the pool of LD in metastatic breast cancer cells

Previously, formation of lipid droplets has been shown to be required for formation of brain metastases in several types of cancer (68). Together with our *in vivo* studies, targeting *FABP7* seems to inhibit HER2+ tumor growth in the brain microenvironment by reducing the capacity of these cells to perform both aerobic glycolysis and formation of lipid droplets. These findings are in agreement with previous studies supporting a role for FABP7 in the formation of LD in breast cancer cells in hypoxic conditions (19). Moreover, increased levels of LD correlate with increased survival of breast cancer and glioblastoma cells under both normoxia and hypoxia conditions (19, 33).

In summary, our results suggest a novel role for FABP7 in breast cancer progression, metastasis and survival in the brain microenvironment. We demonstrate that FABP7 expression is required for the adaptation and growth of HER2+ breast cancer cells in the brain microenvironment, acting as a potential switch between oxidative phosphorylation of lipids and formation of lipid droplets. Furthermore, increased FABP7 levels correlate with increased invasive and metastatic properties of HER2+ breast cancer cells. In future studies, it will be important to determine the role of FABP7 in the metastatic potential of other breast cancer cell subtypes, and to determine whether FABP7 plays further mechanistic roles in BCBM formation. Given the present results, FABP7 is a potential biomarker for increased risk of brain metastases in HER2+ breast cancer patients and future efforts should aim to develop mechanisms to target FABP7 in HER2+ breast cancer patients to prevent and/or treat BCBM.

MATERIALS AND METHODS

Additional materials and methods can be found in the Supplemental Information available at Oncogene's website.

Cell culture and reagents

Breast cancer cell lines BT474 and BT474-Br (20), kindly provided by Dr. Dihua Yu (MD Anderson Cancer Center) were maintained in DMEM 10% fetal bovin serum (FBS). HCC1569 and HCC1954 (Dr. Olopade, University of Chicago) were maintained in RPMI 10% FBS. See supplemental information for an extended cell culture description.

For lentiviral transduction, non-target control shRNA and 2 different shRNA specific to *FABP7* were procured (Sigma, MO, USA) (Supplementary Table S1). pCS6 lentiviral vector containing full-length *FABP7* was used to overexpress *FABP7* in breast cancer cells (#BC012299, TransOMIC). Lentiviral particles were generated as in previous studies (24). (see supplemental information for a detailed description of the antibody used)

Animal experiments

All surgical procedures were conducted in accordance with NIH guidelines on the care and use of laboratory animals for research purposes. The Institutional Committee on Animal Use at Northwestern University approved the protocols. Animal procedures were performed as in our previous studies (24, 69) (see supplemental information for a detailed description)

Western blotting and Immunofluorescence

Equal amounts of total cell lysates were resolved by SDS-PAGE and processed for western blotting essentially as in our previous studies (24, 69). Immunofluorescence staining for FABP7 was conducted as previously described (69). See supplemental information for a detailed description

Quantitative real-time PCR

RNA isolation from breast cancer cells, cDNA reverse-transcription and qRTPCR were conducted as in previous studies (24) using the primers indicated in Supplementary Table S2.

Invasion assay

Matrigel invasion assays were conducted using Biocoat Matrigel invasion chambers (5×10^4 cells/insert) as in our previous studies (24).

OCR and ECAR analysis

Extracellular flux analyses measuring OCR and ECAR were performed using the Mito Stress test protocol developed by Agilent/Seahorse Biosciences (Santa Clara, CA, USA), and measured in the Seahorse Xfe96 analyzer. Results were analyzed using the Agilent's Wave software. See supplemental information for a detailed description.

Fatty acid oxidation assay and Lipid droplet quantification

Analyses of the fatty acid oxidation rate of breast cancer cells were performed using the Agilent/Seahorse mitochondrial stress test assay modified with an initial lipidic injection with palmitate-BSA (Agilent/Seahorse Biosciences) or oleate-BSA (Sigma, MO, USA) as in our previous studies (70). LD detection was performed as previously described (71), and LD quantification was carried out as described in the supplemental information.

Statistical Analysis

All statistical analyses were performed using GraphPad Prism 7.03 (Graphpad Software, Inc). Student's t-test was used for comparisons between two groups. One-way analysis of variance (ANOVA) was used to compare more than two groups followed by Tukey's test. Survival curves were generated by Kaplan–Meier, and the log-rank test was used to compare the distributions of survival time. Recursive partitioning analysis (22) was used to establish an optimal cut-off point of FABP7 expression for predicting survival in breast cancer patients (see supplemental information for a detailed description). Results are representative of three independent experiments, and bar graphs represent means ± SD unless otherwise specified. Normality assumption was checked by using Shapiro-Wilk test with Quantile-Quantile plots and equal variance assumption was checked by using Brown-Forsythe test together with residual plot for continuous variables. Sample size was determined based on similar experiments in previous publications. p values <0.05 were considered statistically significant.

Supplementary Material

Refer to Web version on PubMed Central for supplementary material.

ACKNOWLEDGEMENTS

REFERENCES

1. Leyland-Jones B Human epidermal growth factor receptor 2-positive breast cancer and central nervous system metastases. J Clin Oncol. 2009;27(31):5278–86. [PubMed: 19770385]

2. Kodack DP, Askoxylakis V, Ferraro GB, Fukumura D, Jain RK. Emerging strategies for treating brain metastases from breast cancer. Cancer Cell. 2015;27(2):163–75. [PubMed: 25670078]

3. Blackwell KL, Burstein HJ, Storniolo AM, Rugo HS, Sledge G, Aktan G, et al. Overall survival benefit with lapatinib in combination with trastuzumab for patients with human epidermal growth factor receptor 2-positive metastatic breast cancer: final results from the EGF104900 Study. J Clin Oncol. 2012;30(21):2585–92. [PubMed: 22689807]

4. Slamon DJ, Clark GM, Wong SG, Levin WJ, Ullrich A, McGuire WL. Human breast cancer: correlation of relapse and survival with amplification of the HER-2/neu oncogene. Science. 1987;235(4785):177–82. [PubMed: 3798106]

5. Emi Y, Kitamura K, Shikada Y, Kakeji Y, Takahashi I, Tsutsui S. Metastatic breast cancer with HER2/neu-positive cells tends to have a morbid prognosis. Surgery. 2002;131(1 Suppl):S217–21. [PubMed: 11821814]

6. Gajria D, Chandarlapaty S. HER2-amplified breast cancer: mechanisms of trastuzumab resistance and novel targeted therapies. Expert Rev Anticancer Ther. 2011;11(2):263–75. [PubMed: 21342044]

7. Bos PD, Zhang XH, Nadal C, Shu W, Gomis RR, Nguyen DX, et al. Genes that mediate breast cancer metastasis to the brain. Nature. 2009;459(7249):1005–9. [PubMed: 19421193]

8. Sihto H, Lundin J, Lundin M, Lehtimaki T, Ristimaki A, Holli K, et al. Breast cancer biological subtypes and protein expression predict for the preferential distant metastasis sites: a nationwide cohort study. Breast Cancer Res. 2011;13(5):R87. [PubMed: 21914172]

9. Neman J, Termini J, Wilczynski S, Vaidehi N, Choy C, Kowolik CM, et al. Human breast cancer metastases to the brain display GABAergic properties in the neural niche. Proc Natl Acad Sci U S A. 2014.

10. Valiente M, Obenauf AC, Jin X, Chen Q, Zhang XH, Lee DJ, et al. Serpins promote cancer cell survival and vascular co-option in brain metastasis. Cell. 2014;156(5):1002–16. [PubMed: 24581498]

11. DeBerardinis RJ, Chandel NS. Fundamentals of cancer metabolism. Sci Adv. 2016;2(5):e1600200. [PubMed: 27386546]

12. Seyfried TN, Kiebish MA, Marsh J, Shelton LM, Huysentruyt LC, Mukherjee P. Metabolic management of brain cancer. Biochim Biophys Acta. 2011;1807(6):577–94. [PubMed: 20804725]

13. Thupari JN, Pinn ML, Kuhajda FP. Fatty acid synthase inhibition in human breast cancer cells leads to malonyl-CoA-induced inhibition of fatty acid oxidation and cytotoxicity. Biochem Biophys Res Commun. 2001;285(2):217–23. [PubMed: 11444828]

14. Camarda R, Zhou AY, Kohnz RA, Balakrishnan S, Mahieu C, Anderton B, et al. Inhibition of fatty acid oxidation as a therapy for MYC-overexpressing triple-negative breast cancer. Nat Med. 2016;22(4):427–32. [PubMed: 26950360]

15. Park JH, Vithayathil S, Kumar S, Sung PL, Dobrolecki LE, Putluri V, et al. Fatty Acid Oxidation-Driven Src Links Mitochondrial Energy Reprogramming and Oncogenic Properties in Triple-Negative Breast Cancer. Cell Rep. 2016;14(9):2154–65. [PubMed: 26923594]

16. Wang T, Fahrmann JF, Lee H, Li YJ, Tripathi SC, Yue C, et al. JAK/STAT3-Regulated Fatty Acid beta-Oxidation Is Critical for Breast Cancer Stem Cell Self-Renewal and Chemoresistance. Cell Metab. 2018;27(6):1357.

17. Pascual G, Avgustinova A, Mejetta S, Martin M, Castellanos A, Attolini CS, et al. Targeting metastasis-initiating cells through the fatty acid receptor CD36. Nature. 2017;541(7635):41–5. [PubMed: 27974793]

18. Storch J, Corsico B. The emerging functions and mechanisms of mammalian fatty acid-binding proteins. Annu Rev Nutr. 2008;28:73–95. [PubMed: 18435590]

19. Bensaad K, Favaro E, Lewis CA, Peck B, Lord S, Collins JM, et al. Fatty acid uptake and lipid storage induced by HIF-1alpha contribute to cell growth and survival after hypoxia-reoxygenation. Cell Rep. 2014;9(1):349–65. [PubMed: 25263561]

20. van de Vijver MJ, He YD, van't Veer LJ, Dai H, Hart AA, Voskuil DW, et al. A gene-expression signature as a predictor of survival in breast cancer. N Engl J Med. 2002;347(25):1999–2009. [PubMed: 12490681]

21. Zhang XH, Wang Q, Gerald W, Hudis CA, Norton L, Smid M, et al. Latent bone metastasis in breast cancer tied to Src-dependent survival signals. Cancer Cell. 2009;16(1):67–78. [PubMed: 19573813]

22. Lamborn KR, Chang SM, Prados MD. Prognostic factors for survival of patients with glioblastoma: recursive partitioning analysis. Neuro Oncol. 2004;6(3):227–35. [PubMed: 15279715]

23. Zhang S, Huang WC, Zhang L, Zhang C, Lowery FJ, Ding Z, et al. SRC family kinases as novel therapeutic targets to treat breast cancer brain metastases. Cancer Res. 2013;73(18):5764–74. [PubMed: 23913825]

24. Kanojia D, Morshed RA, Zhang L, Miska JM, Qiao J, Kim JW, et al. betaIII-Tubulin Regulates Breast Cancer Metastases to the Brain. Mol Cancer Ther. 2015;14(5):1152–61. [PubMed: 25724666]

25. Krakhmal NV, Zavyalova MV, Denisov EV, Vtorushin SV, Perelmuter VM. Cancer Invasion: Patterns and Mechanisms. Acta Naturae. 2015;7(2):17–28. [PubMed: 26085941]

26. Slipicevic A, Jorgensen K, Skrede M, Rosnes AK, Troen G, Davidson B, et al. The fatty acid binding protein 7 (FABP7) is involved in proliferation and invasion of melanoma cells. BMC Cancer. 2008;8:276. [PubMed: 18826602]

27. Martin TA, Jiang WG. Loss of tight junction barrier function and its role in cancer metastasis. Biochim Biophys Acta. 2009;1788(4):872–91. [PubMed: 19059202]

28. Dong G, Mao Q, Xia W, Xu Y, Wang J, Xu L, et al. PKM2 and cancer: The function of PKM2 beyond glycolysis. Oncol Lett. 2016;11(3):1980–6. [PubMed: 26998110]

29. Pelletier M, Billingham LK, Ramaswamy M, Siegel RM. Extracellular flux analysis to monitor glycolytic rates and mitochondrial oxygen consumption. Methods Enzymol. 2014;542:125–49. [PubMed: 24862264]

30. Reily C, Mitchell T, Chacko BK, Benavides G, Murphy MP, Darley-Usmar V. Mitochondrially targeted compounds and their impact on cellular bioenergetics. Redox Biol. 2013;1(1):86–93. [PubMed: 23667828]

31. Kim HM, Jung WH, Koo JS. Site-specific metabolic phenotypes in metastatic breast cancer. J Transl Med. 2014;12:354. [PubMed: 25496516]

32. Muz B, de la Puente P, Azab F, Azab AK. The role of hypoxia in cancer progression, angiogenesis, metastasis, and resistance to therapy. Hypoxia (Auckl). 2015;3:83–92. [PubMed: 27774485]

33. Koizume S, Miyagi Y. Lipid Droplets: A Key Cellular Organelle Associated with Cancer Cell Survival under Normoxia and Hypoxia. Int J Mol Sci. 2016;17(9).

34. Mitra SK, Schlaepfer DD. Integrin-regulated FAK-Src signaling in normal and cancer cells. Curr Opin Cell Biol. 2006;18(5):516–23. [PubMed: 16919435]

35. LaGory EL, Giaccia AJ. The ever-expanding role of HIF in tumour and stromal biology. Nat Cell Biol. 2016;18(4):356–65. [PubMed: 27027486]

36. Gilkes DM, Bajpai S, Chaturvedi P, Wirtz D, Semenza GL. Hypoxia-inducible factor 1 (HIF-1) promotes extracellular matrix remodeling under hypoxic conditions by inducing P4HA1, P4HA2, and PLOD2 expression in fibroblasts. J Biol Chem. 2013;288(15):10819–29. [PubMed: 23423382]

37. Zhou Y, Jin G, Mi R, Zhang J, Zhang J, Xu H, et al. Knockdown of P4HA1 inhibits neovascularization via targeting glioma stem cell-endothelial cell transdifferentiation and disrupting vascular basement membrane. Oncotarget. 2017;8(22):35877–89. [PubMed: 28415787]

38. Ciminera AK, Jandial R, Termini J. Metabolic advantages and vulnerabilities in brain metastases. Clin Exp Metastasis. 2017;34(6–7):401–10. [PubMed: 29063238]

39. Feng L, Hatten ME, Heintz N. Brain lipid-binding protein (BLBP): a novel signaling system in the developing mammalian CNS. Neuron. 1994;12(4):895–908. [PubMed: 8161459]

40. Haunerland NH, Spener F. Fatty acid-binding proteins--insights from genetic manipulations. Prog Lipid Res. 2004;43(4):328–49. [PubMed: 15234551]

41. Anthony TE, Mason HA, Gridley T, Fishell G, Heintz N. Brain lipid-binding protein is a direct target of Notch signaling in radial glial cells. Genes Dev. 2005;19(9):1028–33. [PubMed: 15879553]

42. Tang Z, Shen Q, Xie H, Zhou X, Li J, Feng J, et al. Elevated expression of FABP3 and FABP4 cooperatively correlates with poor prognosis in non-small cell lung cancer (NSCLC). Oncotarget. 2016;7(29):46253–62. [PubMed: 27323829]

43. Guaita-Esteruelas S, Guma J, Masana L, Borras J. The peritumoural adipose tissue microenvironment and cancer. The roles of fatty acid binding protein 4 and fatty acid binding protein 5. Mol Cell Endocrinol. 2018;462(Pt B):107–18. [PubMed: 28163102]

44. Liang Y, Diehn M, Watson N, Bollen AW, Aldape KD, Nicholas MK, et al. Gene expression profiling reveals molecularly and clinically distinct subtypes of glioblastoma multiforme. Proc Natl Acad Sci U S A. 2005;102(16):5814–9. [PubMed: 15827123]

45. Kaloshi G, Mokhtari K, Carpentier C, Taillibert S, Lejeune J, Marie Y, et al. FABP7 expression in glioblastomas: relation to prognosis, invasion and EGFR status. J Neurooncol. 2007;84(3):245–8. [PubMed: 17415524]

46. Seliger B, Lichtenfels R, Atkins D, Bukur J, Halder T, Kersten M, et al. Identification of fatty acid binding proteins as markers associated with the initiation and/or progression of renal cell carcinoma. Proteomics. 2005;5(10):2631–40. [PubMed: 15892167]

47. Hao J, Zhang Y, Yan X, Yan F, Sun Y, Zeng J, et al. Circulating Adipose Fatty Acid Binding Protein Is a New Link Underlying Obesity-Associated Breast/Mammary Tumor Development. Cell Metab. 2018;28(5):689–705 e5. [PubMed: 30100196]

48. Hao J, Yan F, Zhang Y, Triplett A, Zhang Y, Schultz DA, et al. Expression of Adipocyte/Macrophage Fatty Acid-Binding Protein in Tumor-Associated Macrophages Promotes Breast Cancer Progression. Cancer Res. 2018;78(9):2343–55. [PubMed: 29437708]

49. Pascual G, Dominguez D, Benitah SA. The contributions of cancer cell metabolism to metastasis. Dis Model Mech. 2018;11(8).

50. Liu RZ, Graham K, Glubrecht DD, Lai R, Mackey JR, Godbout R. A fatty acid-binding protein 7/RXRbeta pathway enhances survival and proliferation in triple-negative breast cancer. J Pathol. 2012;228(3):310–21. [PubMed: 22322885]

51. Zhang Y, Sun Y, Rao E, Yan F, Li Q, Zhang Y, et al. Fatty acid-binding protein E-FABP restricts tumor growth by promoting IFN-beta responses in tumor-associated macrophages. Cancer Res. 2014;74(11):2986–98. [PubMed: 24713431]

52. Stivarou T, Patsavoudi E. Extracellular molecules involved in cancer cell invasion. Cancers (Basel). 2015;7(1):238–65. [PubMed: 25629807]

53. Thakur R, Trivedi R, Rastogi N, Singh M, Mishra DP. Inhibition of STAT3, FAK and Src mediated signaling reduces cancer stem cell load, tumorigenic potential and metastasis in breast cancer. Sci Rep. 2015;5:10194. [PubMed: 25973915]

54. Feng Y, Spezia M, Huang S, Yuan C, Zeng Z, Zhang L, et al. Breast cancer development and progression: Risk factors, cancer stem cells, signaling pathways, genomics, and molecular pathogenesis. Genes Dis. 2018;5(2):77–106. [PubMed: 30258937]

55. Chlenski A, Ketels KV, Korovaitseva GI, Talamonti MS, Oyasu R, Scarpelli DG. Organization and expression of the human zo-2 gene (tjp-2) in normal and neoplastic tissues. Biochim Biophys Acta. 2000;1493(3):319–24. [PubMed: 11018256]

56. Liu KC, Cheney RE. Myosins in cell junctions. Bioarchitecture. 2012;2(5):158–70. [PubMed: 22954512]

57. Chua J, Rikhy R, Lippincott-Schwartz J. Dynamin 2 orchestrates the global actomyosin cytoskeleton for epithelial maintenance and apical constriction. Proc Natl Acad Sci U S A. 2009;106(49):20770–5. [PubMed: 19948954]

58. Bennett V, Healy J. Membrane domains based on ankyrin and spectrin associated with cell-cell interactions. Cold Spring Harb Perspect Biol. 2009;1(6):a003012. [PubMed: 20457566]

59. Martin TA, Watkins G, Mansel RE, Jiang WG. Loss of tight junction plaque molecules in breast cancer tissues is associated with a poor prognosis in patients with breast cancer. Eur J Cancer. 2004;40(18):2717–25. [PubMed: 15571953]

60. Marie SK, Shinjo SM. Metabolism and brain cancer. Clinics (Sao Paulo). 2011;66 Suppl 1:33–43. [PubMed: 21779721]

61. Han T, Kang D, Ji D, Wang X, Zhan W, Fu M, et al. How does cancer cell metabolism affect tumor migration and invasion? Cell Adh Migr. 2013;7(5):395–403. [PubMed: 24131935]

62. Gatenby RA, Gawlinski ET, Gmitro AF, Kaylor B, Gillies RJ. Acid-mediated tumor invasion: a multidisciplinary study. Cancer Res. 2006;66(10):5216–23. [PubMed: 16707446]

63. Talasila KM, Rosland GV, Hagland HR, Eskilsson E, Flones IH, Fritah S, et al. The angiogenic switch leads to a metabolic shift in human glioblastoma. Neuro Oncol. 2017;19(3):383–93. [PubMed: 27591677]

64. Desai S, Ding M, Wang B, Lu Z, Zhao Q, Shaw K, et al. Tissue-specific isoform switch and DNA hypomethylation of the pyruvate kinase PKM gene in human cancers. Oncotarget. 2014;5(18): 8202–10. [PubMed: 24077665]

65. Nguyen A, Loo JM, Mital R, Weinberg EM, Man FY, Zeng Z, et al. PKLR promotes colorectal cancer liver colonization through induction of glutathione synthesis. J Clin Invest. 2016;126(2): 681–94. [PubMed: 26784545]

66. Beloribi-Djefaflia S, Vasseur S, Guillaumond F. Lipid metabolic reprogramming in cancer cells. Oncogenesis. 2016;5:e189. [PubMed: 26807644]

67. Cheng C, Edin NF, Lauritzen KH, Aspmodal I, Christoffersen S, Jian L, et al. Alterations of monocarboxylate transporter densities during hypoxia in brain and breast tumour cells. Cell Oncol (Dordr). 2012;35(3):217–27. [PubMed: 22700320]

68. Sjobakk TE, Vettukattil R, Gulati M, Gulati S, Lundgren S, Gribbestad IS, et al. Metabolic profiles of brain metastases. Int J Mol Sci. 2013;14(1):2104–18. [PubMed: 23340650]

69. Kanojia D, Balyasnikova IV, Morshed RA, Frank RT, Yu D, Zhang L, et al. Neural Stem Cells Secreting Anti-HER2 Antibody Improve Survival in a Preclinical Model of HER2 Overexpressing Breast Cancer Brain Metastases. Stem Cells. 2015;33(10):2985–94. [PubMed: 26260958]

70. Miska J, Lee-Chang C, Rashidi A, Muroski ME, Chang AL, Lopez-Rosas A, et al. HIF-1alpha Is a Metabolic Switch between Glycolytic-Driven Migration and Oxidative Phosphorylation-Driven Immunosuppression of Tregs in Glioblastoma. Cell Rep. 2019;27(1):226–37 e4. [PubMed: 30943404]

71. Listenberger LL, Studer AM, Brown DA, Wolins NE. Fluorescent Detection of Lipid Droplets and Associated Proteins. Curr Protoc Cell Biol. 2016;71:4.31.1–4.14. [PubMed: 27245427]

72. Enerly E, Steinfeld I, Kleivi K, Leivonen SK, Aure MR, Russnes HG, et al. miRNA-mRNA integrated analysis reveals roles for miRNAs in primary breast tumors. PLoS One. 2011;6(2):e16915. [PubMed: 21364938]
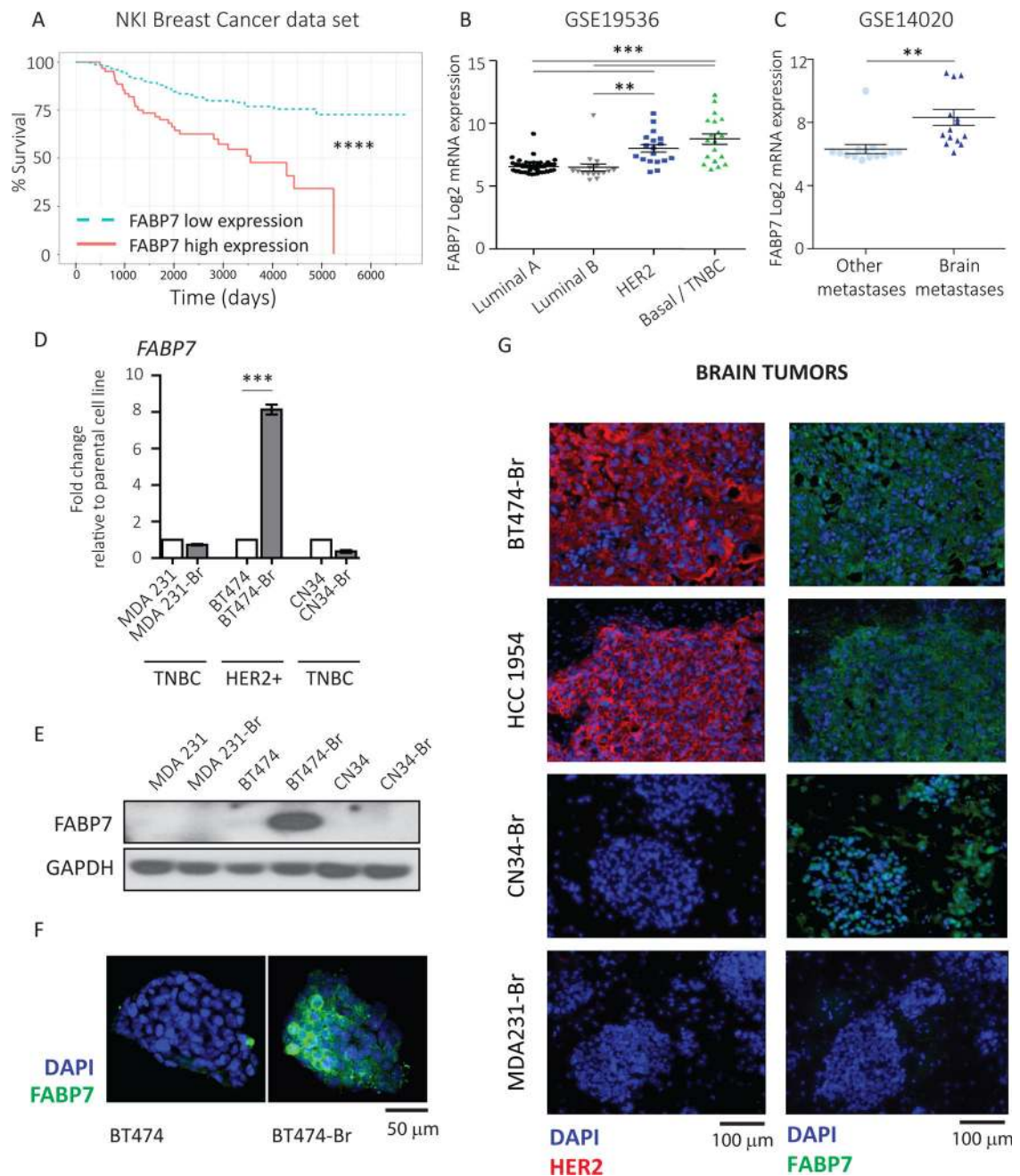
Figure 1. Increased levels of FABP7 correlate with poor survival in breast cancer patients and greater incidence of brain metastases in HER2+ breast cancer.

A) Kaplan Meier survival curves showing percent of survival between breast cancer patients with high (n=61) versus low (n=227) expression levels of FABP7. Data were extracted from NKI Breast Cancer database (20). B) FABP7 relative gene expression levels are shown for patients in Luminal A (n=45), Luminal B (n=16), HER2+ (n=18) and Basal/TNBC (n=16) breast cancer patients, as indicated, using *Enerly E. et.al* (72) data set (GSE19536). C) FABP7 relative gene expression levels are shown in metastasis to other organs (lung, bone) (n=14) versus metastasis to the brain (n=14) in breast cancer patients using *Zhang XH. et. al.* (21) data set (GSE14020). C-E) Expression of FABP7 levels in TNBC (MDA231, CN34)

and HER2+ breast cancer (BT474) cells and their brain metastatic (Br) counterparts. D) Quantitative RT-PCR analyses of the relative mRNA expression of FABP7, normalized to GAPDH levels, is shown for the indicated cell lines. Data are expressed as fold change over respective parental cell line. Results are representative of three independent experiments, and bar graphs represent means ± SD. E) The indicated cell lines were lysed and equal amounts of whole-cell lysates were resolved by SDS-PAGE. Immunoblots were probed with antibodies against FABP7 and GAPDH (loading control). Immunoblot images are representative of three independent experiments. F) Representative immunofluorescence pictures, from three independent experiments, showing FABP7 expression (green) in the indicated cells. Nuclear staining is shown in blue (DAPI). G) Representative immunofluorescence pictures of brain sections harvested from mice injected intracranially with the indicated cell lines (n = 5 per cell line). HER2 staining is shown in red, FABP7 staining is shown in green and nuclear staining is shown in blue (DAPI). Statistical analyses were performed using log rank test (A), two-tailed t-test (C) and one-way ANOVA with post-hoc Tukey's test (B, D): **** p<0.0001; *** p<0.001; ** p<0.01.
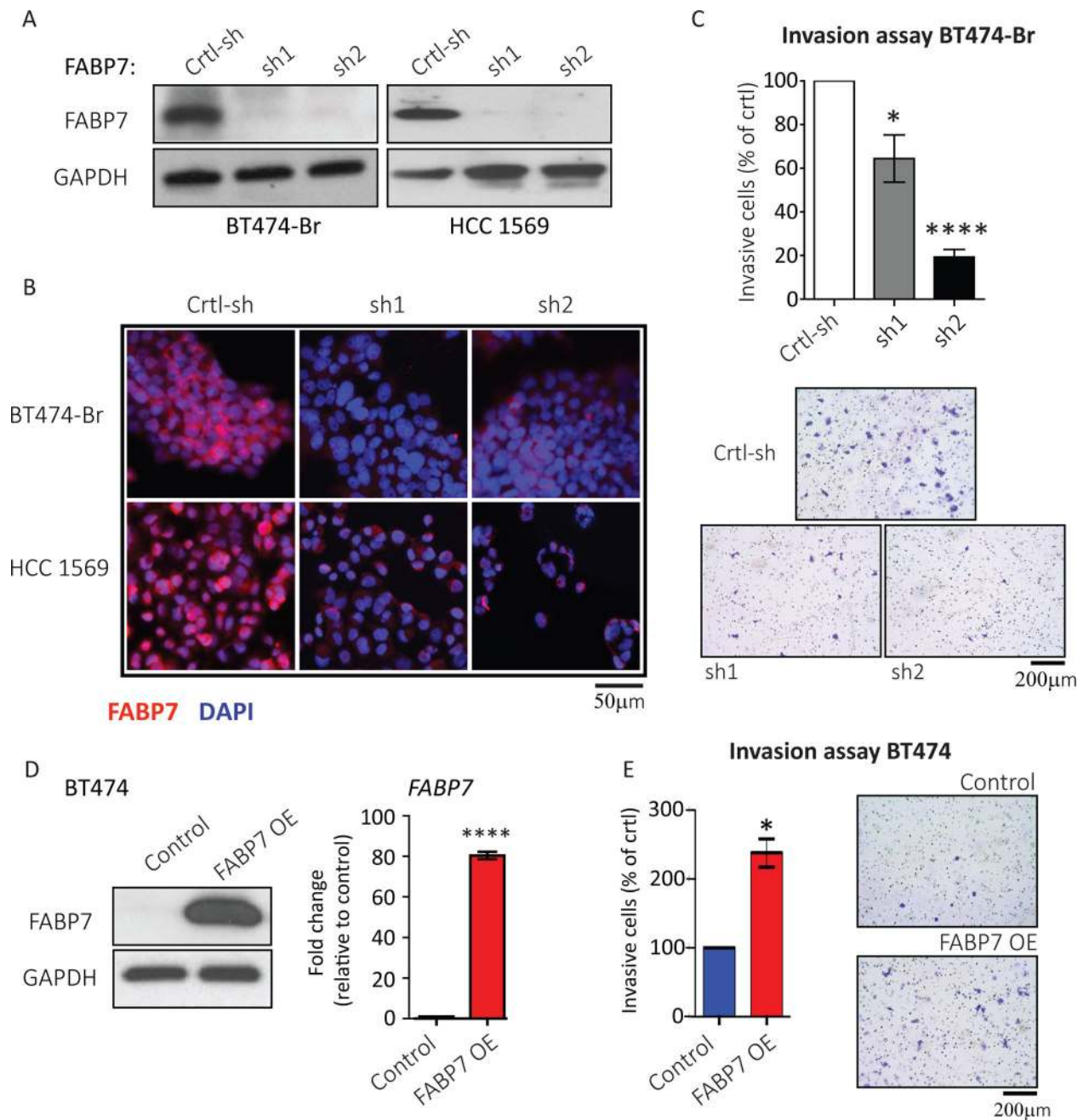
Figure 2. FABP7 is required for HER2+ breast cancer cells invasion *in vitro*.
(A-C) BT474-Br and HCC1569 HER2+ breast cancer cells were transduced with non-target control shRNA (Crtl-sh) or with two distinct specific shRNAs targeting *FABP7* (sh1 and sh2) and stable clones were selected to generate *FABP7* knockdown (KD) (sh1 and sh2) BT474-Br and HCC1569 cells, as indicated. A) Stable cells were lysed and equal amounts of whole-cell lysates were resolved by SDS-PAGE, as indicated. Immunoblots were probed with antibodies against FABP7 and GAPDH (loading control). Immunoblot images are representative of three independent experiments. B) Representative immunofluorescence pictures, from three independent experiments, showing FABP7 expression (red) in the

indicated cells. Nuclear staining is shown in blue (DAPI). C) BT474-Br control (Ctrl-sh) and *FABP7* KD (sh1 and sh2) cells were subjected to invasion assays, and cells that invaded through the matrigel-coated transwell inserts were stained and counted. (top panel) Data are expressed as percent of invasive cells over control and bar graphs represent means ± SD. (bottom panel) Representative images are shown. D-E) HER2+ BT474 breast cancer cells were transduced with control vector (Control) or FABP7 plasmid and stable clones were selected to generate *FABP7* overexpressing (OE) BT474 cells. D) (left panel) Stable cells were lysed and equal amounts of whole-cell lysates were resolved by SDS-PAGE, as indicated. Immunoblots were probed with antibodies against FABP7 and GAPDH (loading control). Immunoblot images are representative of three independent experiments. (right panel) Quantitative RT-PCR analyses of the relative mRNA expression of FABP7, normalized to GAPDH levels, is shown for the indicated cells. Data are expressed as fold change over Control cells. Results are representative of three independent experiments, and bar graphs represent means ± SD. E) BT474 Control and *FABP7* OE cells were subjected to invasion assays and cells that invaded through the matrigel-coated transwell inserts were stained and counted. (left panel) Data are expressed as percent of invasive cells over Control, and bar graphs represent means ± SD. (right panel) Representative images are shown. Statistical analyses were performed using one-way ANOVA with post-hoc Tukey's test (C) and two-tailed t-test (D,E): **** p<0.0001; * p<0.05.
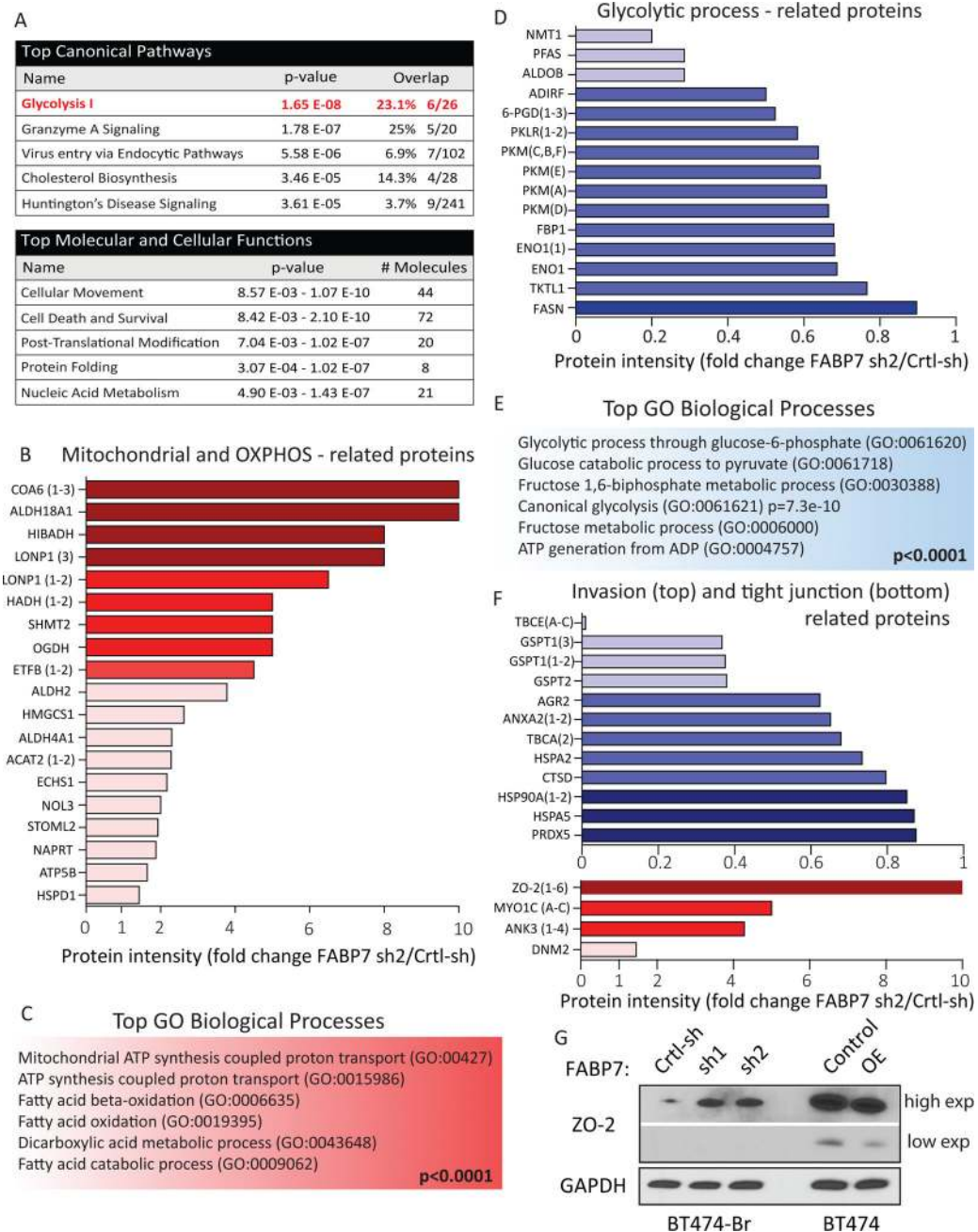
Figure 3. FABP7 is essential for expression of metabolic and invasion-related proteins in HER2+ BCBM cells.

A-F) Total protein extracts from control BT474-Br (Ctrl-sh) and *FABP7* KD BT474-Br (FABP7 sh2) cells were subjected to LC-MS/MS analysis using LTQ-Orbitrap. From the 8687 total proteins identified, 256 proteins were significantly differentially expressed in *FABP7* KD BT474-Br cells compared to control cells. Ingenuity® gene ontology (GO) analysis of the 256 proteins differentially expressed between *FABP7* KD BT474-Br cells and control cells was performed. A) Tables show the top 5 canonical pathways and molecular and cellular functions altered in *FABP7* KD BT474-Br cells compared to control cells. B) Fold change increased expression levels of proteins related with mitochondrial

function in *FABP7* KD BT474-Br cells over control cells. C) GO term analysis was used to identify enriched biological processes. Table shows the top 6 biological processes up-regulated in *FABP7* KD BT474-Br cells compared to control cells. D) Fold change decreased expression levels of proteins related with the glycolytic process in *FABP7* KD BT474-Br cells over control cells. E) GO term analysis was used to identify enriched biological processes. Table shows the top 6 biological processes down-regulated in *FABP7* KD BT474-Br cells compared to control cells. F) Fold change increased expression levels of proteins involved in the tumor cell invasion processes (top) and fold change decreased expression levels of tight junction-related proteins (bottom) in *FABP7* KD BT474-Br cells compared to control cells. G) BT474-Br control (Ctrl-sh), *FABP7* KD BT474-Br (sh1 and sh2), BT474 control (Ctrl), and *FABP7* overexpressing BT474 (OE) cells were lysed and equal amounts of whole-cell lysates were resolved by SDS-PAGE and immunobloted with antibodies against ZO-2 and GAPDH (loading control). High a low exposure (exp) of ZO-2 levels are shown.
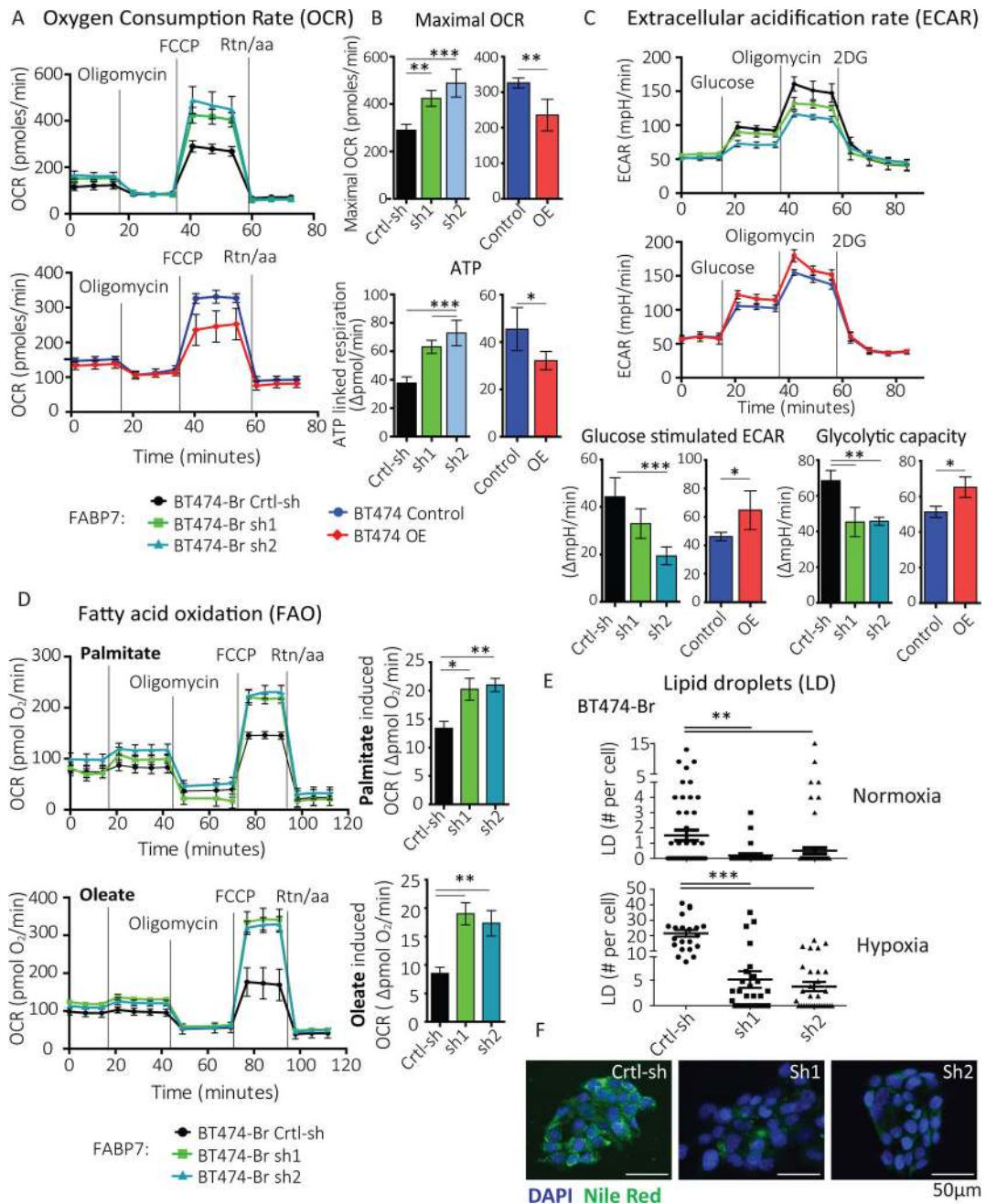
Figure 4. FABP7 regulates the metabolic reprogramming in HER2+ BCBM cells.
(A-B) Time course analysis for the measurement of oxygen consumption rate (OCR) and ATP-linked respiration in BT474-Br control (Ctrl-sh), *FABP7* KD BT474-Br (sh1 and sh2), BT474 control (Control), and *FABP7* overexpressing BT474 (OE) cells. A) Basal OCR conditions are shown, followed by sequential addition of oligomycin (2 μM), FCCP (2 μM) and Rtn/aa (0.5 μM) for the indicated cells. B) (top panel) Maximal OCR levels and (bottom panel) mitochondrial-dependent ATP synthesis in cells was calculated after olygomicin treatment. (A-B) Results are representative of three independent experiments, and bar graphs represent means ± SD. C) Time course analysis for the measurement of the extracellular

acidification rate (ECAR) was performed in BT474-Br control (Ctrl-sh), *FABP7* KD BT474-Br (sh1 and sh2), BT474 control (Control), and *FABP7* overexpressing BT474 (OE) cells grown in hypoxic (1% O_2) conditions for 24h. (top panels) Basal ECAR conditions are shown, followed by sequential injection of glucose (10 mM), oligomycin (1 μM) and 2DG (50 mM). (bottom panels) Glucose stimulated ECAR and Glycolytic capacity in cells were measured after addition of glucose and oligomycin respectively. Results are representative of three independent experiments, and bar graphs represent means ± SD. D) Time course analysis for the measurement of the fatty acid oxidation in BT474-Br control (Ctrl-sh), *FABP7* KD BT474-Br (sh1 and sh2) grown in hypoxic (1% O_2) conditions for 24h. Palmitate-BSA (100 μM) or oleate-BSA (100 μM) were injected to cells, followed by sequential injection of oligomycin (2 μM), FCCP (4 μM) and Rtn/aa (0.5 μM). (bottom panels) Palmitate and oleate-induced OCR in cells were calculated after its injection. Results are representative of three independent experiments, and bar graphs represent means ± SEM. (E-F) Lipid droplet (LD) quantification, based on Nile-Red positive staining, was performed in BT474-Br control (Ctrl-sh) and *FABP7* KD (sh1 and sh2) cells grown in hypoxic (1% O_2) and normoxic (20.7% O_2) conditions for 24h. E) Number of LD per cell based on Nile-Red positive immunostaining (IF). Results are representative of three independent experiments, and bar graphs represent means ± SEM. F) Representative immunofluorescence pictures, from three independent experiments, showing LD levels (green) in the indicated cells. Nuclear staining is shown in blue (DAPI). (A-E) Statistical analysis were performed using one-way ANOVA with post-hoc Tukey's test and two-tailed t-test. *** $p<0.001$; ** $p<0.01$; * $p<0.05$
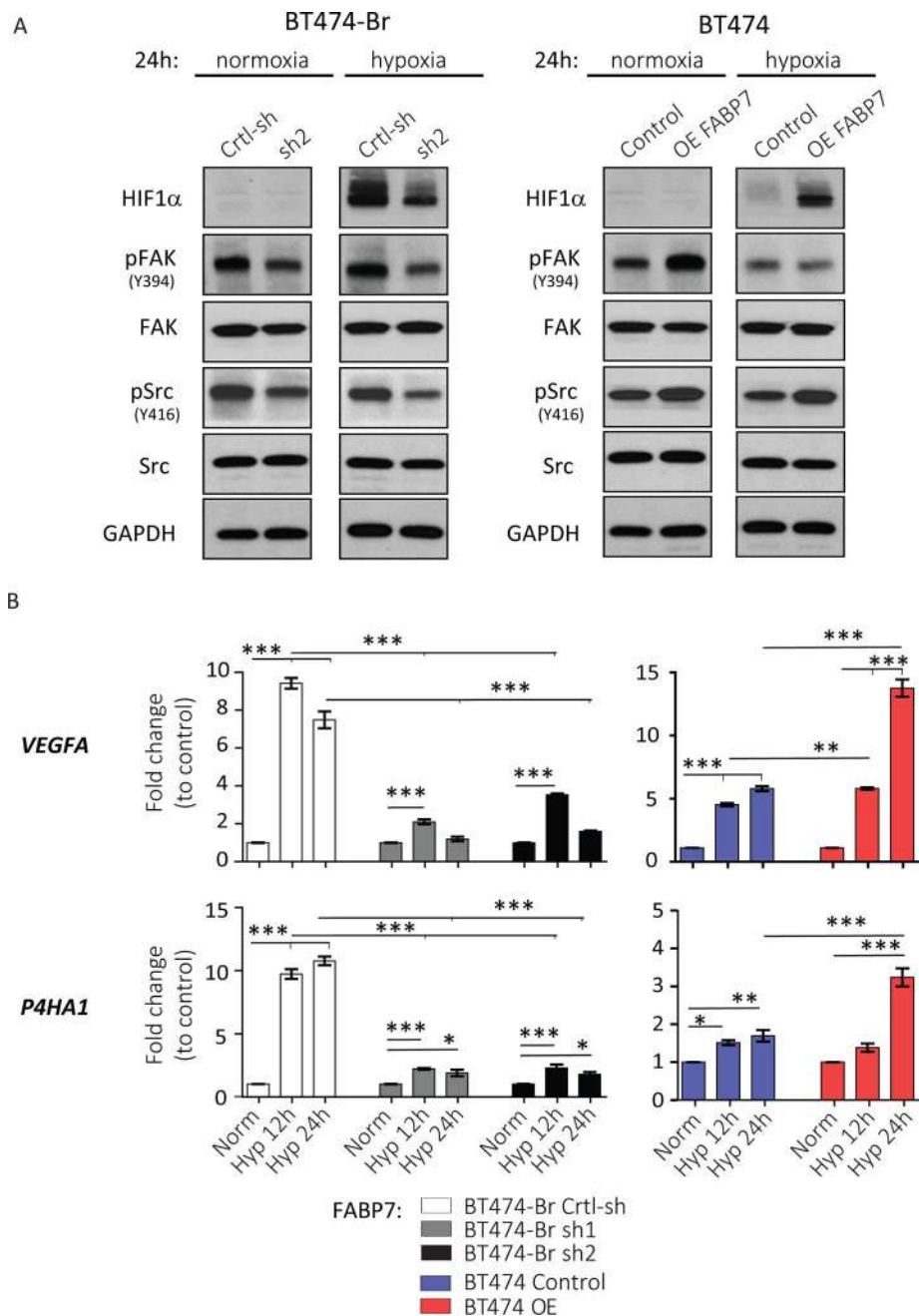
Figure 5. *FABP7* knockdown in HER2+ BCBM cells attenuates the integrin-Src signaling and the expression of proangiogenic factors.
A) BT474-Br control (Ctrl-sh), *FABP7* KD BT474-Br (sh2), BT474 control (Control), and *FABP7* overexpressing BT474 (OE) cells grown in hypoxic (1% O_2) and normoxic (20.7% O_2) conditions for 24h were lysed and equal amounts of whole-cell lysates were resolved by SDS-PAGE. Immunoblots were probed with antibodies against HIF1α, pFAK (phosphorylation at Y394), total FAK, pSrc (phosphorylation at Y416), total Src, and GAPDH (loading control). Immunoblot images are representative of three independent experiments. B) Quantitative RT-PCR analyses of the relative mRNA expression of VEGFA (top) and P4HA1 (bottom), normalized to GAPDH levels, is shown for the indicated cells.

Data are expressed as fold change of hypoxia-treated cells (12h and 24h) over respective normoxic conditions. Results are representative of three independent experiments, and bar graphs represent means ± SD. Statistical analysis were performed using one-way ANOVA with post-hoc Tukey's test. *** p<0.001; ** p<0.01; * p<0.05.
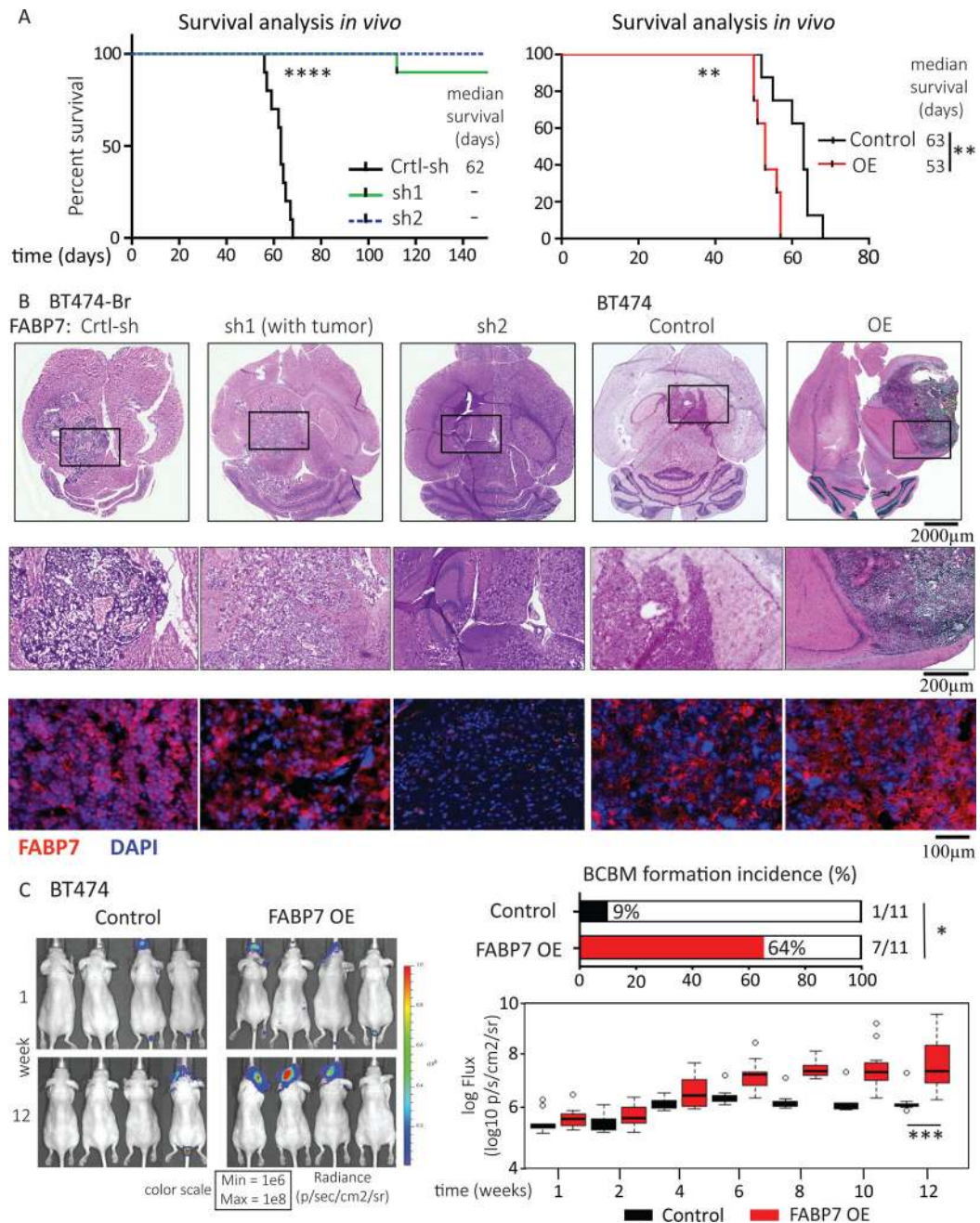
Figure 6. FABP7 is required for the formation of HER2+ breast cancer brain metastases cells *in vivo*.

A-B) BT474-Br control (Ctrl-sh), *FABP7* KD BT474-Br (sh1 and sh2), BT474 control (Control), and *FABP7* overexpressing BT474 (OE) cells were injected intracranially in nude mice (5×10^5 cells/brain), and survival was monitored. A) (left panel) Kaplan Meier graph showing percent of survival between BT474-Br control (Ctrl-sh) and *FABP7* KD BT474-Br (sh1 and sh2) groups. Median survival in BT474-Br control (Ctrl-sh) were 62 days, whereas only one mouse (out of 10) in the *FABP7* sh1 KD BT474-Br group died at day 112. Log rank test was applied to compare mice survival (n=10 per group, **** p<0.0001). (right panel) Kaplan Meier graph showing percent of survival between BT474 control (Ctrl), and

FABP7 overexpressing BT474 (OE) cells (median survival of 53 and 63 days, respectively). Log rank test was applied to compare mice survival (n=8 per group; ** p<0.0039). B) Representative histopathological images (H&E) (top) and immunofluorescence pictures (bottom) of brain sections harvested from mice from the indicated groups. FABP7 staining is shown in red, nuclear staining is shown in blue (DAPI). C) Firefly luciferase-positive BT474 control (Ctrl), and *FABP7* overexpressing BT474 (OE) cells were injected systemically via an intracardiac route (3×10^5 cells/mouse, n=11 per group), and BCBM formation was monitored using bioluminescence imaging (BLI) signals (photons/second). (left panel) Representative firefly luciferase BLI images of BCBM formation in mice from the indicated groups 1 week and 12 weeks after tumor cell injection. Scale bar shows pseudocolor display for photon flux with red and blue representing highest and lowest values, respectively. (right panel) Percentage of BCBM incidence (top) and BLI signal intensity (log10 p/sec/cm2/sr) (bottom, represented as box plot) in mice from the indicated groups at the indicated time points. Statistical analysis were performed using Fisher's exact test (top, * p=0.0237) and two way ANOVA followed by Sidak's test (bottom, *** p<0.001).